This is the accepted version of the article: Van Vörden D.; Wortmann B.; Schmidt N. [et al.]. Following the steps of a reaction by direct imaging of many individual molecules. ***Chemical Communications***, 52(49):2016, p. 7711-7714

Available at: https://doi.org/10.1039/c6cc02959k

Journal Name

ARTICLE TYPE

Cite this: DOI: 10.1039/xxxxxxxxxx

Following the steps of a reaction by direct imaging of many individual molecules

Dennis van Vörden,[a] Ben Wortmann,[a] Nico Schmidt,[a] Manfred Lange,[a] Roberto Robles,[b] Lothar Brendel,[a] Christian A. Bobisch[a] and Rolf Möller[a]

Received Date
Accepted Date

DOI: 10.1039/xxxxxxxxxx

www.rsc.org/journalname

The dehydrogenation and dechlorination of FeOEP-Cl on Cu(111) has been studied in detail by scanning tunneling microscopy. Although, it is not possible to follow the reaction of an individual molecule, the complete pathway of the reaction with 22 inequivalent intermediate states and the rates of the involved processes are revealed. This is achieved by combining the analysis of a large data set showing thousands of molecules in the different stages of the reaction with numerical simulations.

The identification of the reaction pathway and intermediate states of a chemical reaction on a surface is in general a difficult task. In particular, if intermediate species are scarce or almost identical, spectroscopic techniques averaging over the whole surface fail.[1] If the reactant remains at a fixed position while undergoing the chemical reaction scanning tunneling microscopy (STM) and scanning force microscopy can be successfully applied to follow the reaction of individual molecules.[2,3] However, many reactions require an activation causing the molecules to diffuse along the surface. Instead of directly following the reaction, the products can be looked at after reducing the sample temperature. This has been demonstrated for isolated molecules[4–7] and for the formation of networks of organic molecules[8–10]. Marbach *et al.* as well as Wintterlin *et al.* have shown that by looking at an ensemble of molecules the rate for a reaction may be determined for simple reactions.[11,12]

In this paper we show that by monitoring a very large ensemble of molecules, the pathway of a reaction as well as the rates for the different steps can be evaluated for a system with 22 intermediate species and a simple branching scheme. The present study was performed on the 2,3,7,8,12,13,17,18-octaethylporphyrin Fe(III) chloride (FeOEP-Cl) molecule adsorbed on a Cu(111) surface. FeOEP-Cl was demonstrated to be particularly interesting due to its properties as a tunable single molecule magnet making it a candidate for molecular spintronic devices.[13–15] The Cu(111) surface is known to catalyze the dehydrogenation of hydrocarbons at moderate temperature[16,17] so that the stability of FeOEP-Cl was an open question. In preliminary work, we saw that at around 400 K the dehydrogenation of FeOEP-Cl starts and the molecule may lose the chlorine ligand at any stage of the dehydrogenation so that the central Fe atom changes from the +3 to the +2 oxidation state finally leading to the formation of iron-II-tetra-benzo-porphyrin (FeTBP).[18,19] This is accompanied by a change of physical and chemical properties, e.g. different adsorption sites, different diffusion of the molecules as well as a modification of the spin state and the magnetic properties.[13,20] Here, we want to shed further light on the underlying reaction pathway.

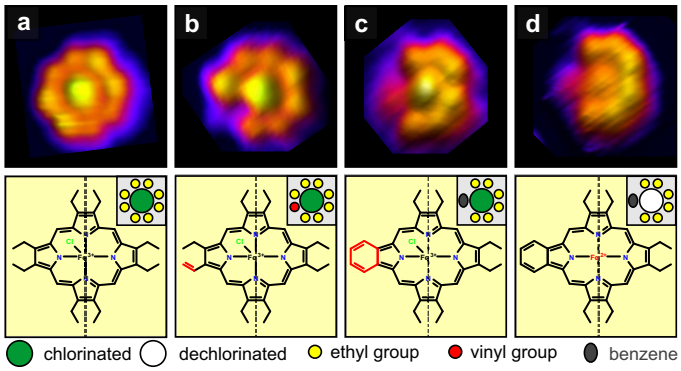

Fig. 1 STM images ($T = 80\ K$, $U = -0.2\ V$, $I = 50\ pA$), structural models and pictograms for different steps of the reaction. (a) initial FeOEP-Cl, (b) vinyl group at an off-axis position, (c) benzene ring at the same position, (d) dechlorinated. The dashed lines indicate the direction of rows of copper atoms.

[a] *University of Duisburg-Essen, Faculty of Physics, Center for Nanointegration Duisburg-Essen, Lotharstrasse 1-21, 47057 Duisburg, Germany. Fax: +49-203-379-1727; Tel: +49-203-379-4220; E-mail: christian.bobisch@uni-due.de, rolf.moeller@uni-due.de*
[b] *Catalan Institute of Nanoscience and Nanotechnology (ICN2), CSIC and The Barcelona Institute of Science and Technology, Campus UAB, Bellaterra, 08193 Barcelona, Spain.*

The first steps of a possible reaction pathway are displayed in Fig.1. (a) shows an STM image, a structural model and a schematic representation of the initial FeOEP-Cl. By dehydrogenation, one ethyl group is transformed to a vinyl group which has a lower apparent height in the STM image (b). Once this reaction has occurred, it is very likely that the neighboring ethyl group will dehydrogenate as well leading to the formation of a benzene ring (c). Like the vinyl-group it appears lower than the ethyl groups. (d) displays the dechlorinated form of (c). The apparent height of the center of the molecule is reduced. However, it should be noted that the dechlorination can happen at any stage of dehydrogenation.

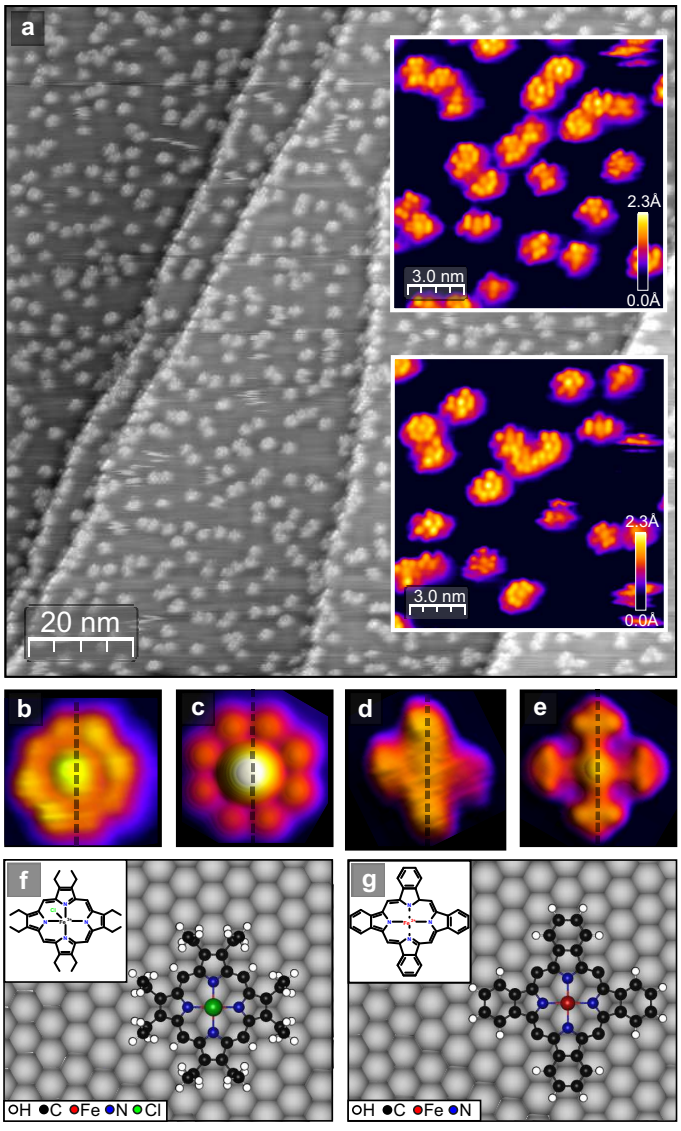

Fig. 2 (a) STM images of a stepped Cu(111) sample showing about 600 molecules after heating to 430 K for 60 min. ($T = 80\ K$, $U = -0.2\ V$, $I = 50\ pA$). The insets show magnifications enabling the differentiation of the states. (b) STM image of FeOEP-Cl , (c) corresponding simulated STM image based on the DFT calculation, (d) STM image of FeTBP, (e) corresponding simulated STM image. At the bottom of the figure the relaxed structures according to the DFT calculations for FeOEP-Cl(f) and FeTBP(g) are shown. The dashed lines in (b)-(e) indicate the axis of the molecule which is aligned to the substrate.

To analyze the complete chemical pathway from FeOEP-Cl to FeTBP in detail the sample was prepared by depositing a submonolayer FeOEP-Cl onto a clean Cu(111) surface, while the sample was kept at room temperature. This results in a distribution of 65% FeOEP-Cl vs. 35% FeOEP on the Cu(111) terraces.[18] To induce the dehydrogenation and dechlorination the sample was heated to 430 K for 1 hour resulting in a broad distribution of the population of all states - initial, intermediate and final. To evaluate the relative population of these states the sample is cooled to 80 K, immobilizing the molecules on the surface. High resolution STM images were acquired allowing us to unambiguously identify the intermediate states for a large number of molecules. Fig.2 displays an STM image of about 600 molecules. The two insets are magnifications of two smaller areas of the same image showing that the different molecular states can be clearly identified. Even though there appears to be some tendency for clusterization there is no evidence for the formation of chemical bonds between the molecules. Adjacent molecules have the same appearance as individually adsorbed molecules so this has no influence on our analysis. For comparison, STM images and the result of DFT calculations of the initial and the final molecule are displayed below.

As can be seen in Fig.2(f) and (g), at $T = 80\ K$ the molecules are oriented with one axis along a densely packed row of copper atoms of the substrate. Since the Cu(111) surface has a threefold symmetry, the four-fold symmetry of the molecule is reduced by the adsorption. At the given reaction temperature however, the molecules will rotate on the surface and even diffuse over step edges. Therefore, the molecules' adsorption geometry when the sample is cooled down after the reaction does not call for a further differentiation of the molecular states in our model of the reaction pathways.

By analyzing several STM images, such as Fig.2, we could identify the intermediate states for more than 10000 molecules. A first observation is that the number of molecules with two or more vinyl groups is negligible. So to improve clarity they are omitted in Fig.3 which shows the relative occupation of the states in the yellow bar graph. Accordingly the probability to find intermediate states with one vinyl group is lower than to find the corresponding state with the benzene ring formed at that position. So evidently the rate of the ring closure is much higher than that of the formation of a single vinyl group.

Another interesting observation can be made for the intermediate states where three to five ethyl groups are dehydrogenated. There are roughly twice as many molecules with vinyl groups adjacent to a benzene ring than molecules with a vinyl group opposite a benzene ring. This is what can be expected for purely statistical reasons since there are four different constellations possible for an adjacent configuration, but only two for an opposing one. Thus the vinyl group formation does not seem to be influenced by the presence of benzene rings on the molecule. It is therefore very likely that the vinyl group formation rate as well as the ring closure rate is almost identical for all molecular states.

For a more extensive understanding of the complete pathway of the transformation of FeOEP-Cl to FeTBP, the experimental observations are compared to a mathematical model describing the population of every involved state as a function of time.

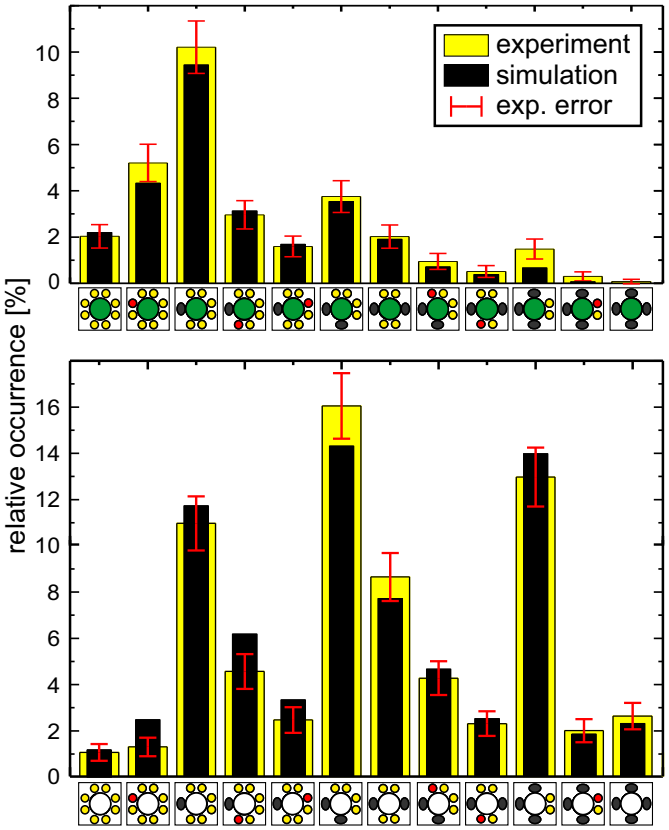

Fig. 3 Relative population of the different states. The experimental results are shown in yellow, the numerical simulation in black. The molecules are sorted by their schematic representation.

Since we deal with a monomolecular reaction, we can use the Polanyi-Wigner-equation of order one to describe the chemical reaction.[21] The rate $R_{ij}(t)$ of transitions $i \to j$ in the system follows:

$$R_{ij}(t) = r_{ij}(t) N_i(t) \tag{1}$$

where $N_i(t)$ is the number of molecules in state i and the transition probability $r_{ij}(t)$ is given by the Arrhenius rate:

$$r_{ij}(t) = \nu_{ij} exp\left(-\frac{E_{ij}}{k_B T}\right). \tag{2}$$

Here ν_{ij} is the attempt frequency, E_{ij} the activation energy, k_B the Boltzmann-constant and T the temperature. The temporal evolution of the number $N_i(t)$ is then given by:

$$\dot{N}_i(t) = \left(\sum_j r_{ji} N_j\right) - \left(N_i \sum_j r_{ij}\right) = \sum_j \Theta_{ij} N_j, \tag{3}$$

with

$$\Theta_{ij} = r_{ji} - \delta_{ij} \sum_k r_{ik} \tag{4}$$

where δ_{ij} is the Kronecker-Symbol.

Hence, we obtain a set of rate equations describing the change of the population of every involved state. Being linear, the same system of ordinary differential equations rules the fractions $n_i(t) \equiv N_i(t)/N_{tot}$ as well. Hence, we can write for $\vec{n}$, the tuple of fractions,

$$\dot{\vec{n}} = \theta \vec{n}. \tag{5}$$

For a fixed temperature T, the matrix θ is constant in time and the solution follows as

$$\vec{n}(t) = exp(t\ \theta) \cdot \vec{n}(0). \tag{6}$$

So far, the description is completely general. The complexity is largely reduced if one can assume that many rates vanish or are negligible. We found that a good agreement between the experiment and a numerical simulation is obtained based on the following assumptions:

1. The rate of dehydrogenation is not influenced by benzene rings that already formed on the same molecule.
2. The rate of dechlorination is independent of the dehydrogenation.
3. The dehydrogenation rates of the chlorinated and the dechlorinated molecules differ only by a constant factor.
4. The transformation occurs stepwise without bypassing intermediate states.

The first assumption follows directly from the experimental observations as described in the preceding paragraphs. The second assumption extends the idea that the dehydrogenation on one arm of the molecule has little effect on the rest of the molecule to the process of dechlorination. The dechlorination of FeOEP-Cl on the other hand has been shown to cause significant changes to the general properties of the molecule.[13,20] Nevertheless, the changes should influence all ethyl groups in the same way which leads to our third assumption. As we did not find any striking experimental evidence against the fourth assumption we may faithfully ad it to greatly decrease the number of fitting parameters and simplify the model. Thus, noting the above exceptions, the assumptions are based on the idea that the different reactions are independent of each other.

All possible reaction paths, starting with the initial state given by the FeOEP-Cl and ending with the FeTBP, are displayed in Fig.4. Since the observed number of molecules with two vinyl groups is negligible they are not included in our model. For a better overview equivalent states have been grouped reducing the system to 22 distinct intermediate states. Equal rates are shown with arrows of the same color. The numbers on the arrows are the statistical weight given by the number of equivalent final states of this reaction step.

Fixing the time unit as the duration t^*, the time the sample is heated to induce the different reactions, only three rates (f_1, f_2, f_3 for vinyl group formation, benzene ring formation, dechlorination) and the ratio c between the dehydrogenation rates of chlorinated and dechlorinated molecules are sufficient to fully capture the reaction. We can determine these four parameters via numerically minimizing:

$$\sum_i \frac{\left(n_i(t^*) - n_{i,exp}\right)^2}{n_i(t^*)} \tag{7}$$

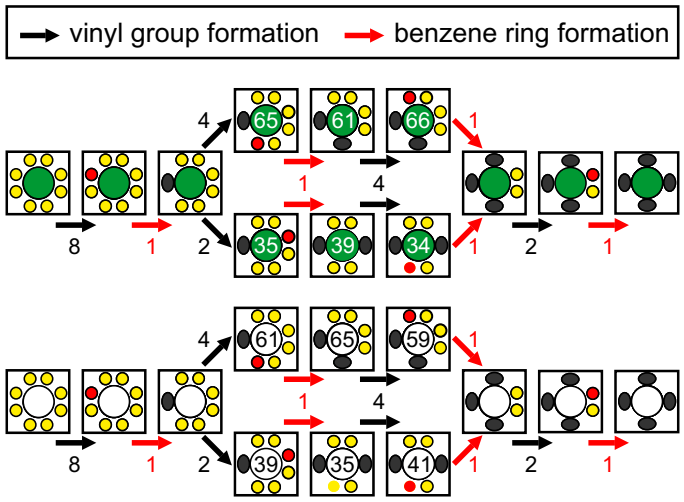

Fig. 4 Scheme of the reaction pathway. The dehydrogenation processes occur within either one of the horizontal strands as indicated by the arrows. The numbers at the arrows mark the statistical weight given by the number of equivalent resulting states. A dechlorination can happen at any time causing a transition from the chlorinated molecule in the top strand to the corresponding dechlorinated one in the same column in the bottom strand. The intermediate states with three to five dehydrogenated ethyl groups can be differentiated by an adjacent or opposite constellation of transformed groups. The numbers in these states correspond to the experimentally obtained distribution in percent.

by means of Powell's method[22], where $\vec{n}_{exp}$ are the experimentally measured fractions. The parameters (f_1, f_2, f_3, c) which provide the best fit to the experimental data are summarized in Tab.1. The corresponding populations of the different states are superimposed on our experimental data in Fig.3 using black bars. The good agreement suggests that the assumptions made above capture the basic features of the reaction.

Table 1 Rates providing the optimal fit to the experimental data. The column to the right gives the difference in activation energy relative to the dechlorination process.

c	dechlor./chlor. rate ratio	1.88 ± 0.03	
	chlorinated molecules	rate (1/h)	ΔE (meV)
f_1	vinyl group formation	0.64 ± 0.01	5 ± 0.7
f_2	benzene ring formation	3.65 ± 0.08	70 ± 0.5
f_3	dechlorination	0.56 ± 0.02	0
	dechlorinated molecules		
cf_1	vinyl group formation	1.20 ± 0.02	28 ± 0.7
cf_2	benzene ring formation	6.86 ± 0.15	93 ± 0.5

Based on the Arrhenius rate (see above), knowing the rates and the temperature, the difference of the activation energy between two processes k and l can be calculated (it is assumed that the attempt frequencies are equal):

$$\Delta E_{kl} = ln\left(\frac{f_k}{f_l}\right) k_B T. \quad (8)$$

The values in Tab.1 are given relative to the dechlorination process (f_3). To obtain the absolute values of the activation energy the time or the temperature for the reaction has to be varied. This was done in a previous work allowing us to estimate the activation energy for the dechlorination to be $1.2 \pm 0.1\ eV$.[19]

In summary, we studied the transformation of FeOEP-Cl to FeTBP, which involves 22 inequivalent intermediate states. The evolution of the population of the states can be described well with just four independent numbers, because the probabilities of the different reactions are independent of each other and are determined only by the very local environment. Previous reactions on other parts of this small molecule do not play a role. This is the case not only for the dehydrogenation of the ethyl groups but also for the dechlorination of the iron core which both are independent of the degree of dehydrogenation of the molecule. However, if the molecule is dechlorinated, the rates for dehydrogenation increase due an enhanced interaction with the supporting substrate.

Our work shows that the different steps of a chemical reaction on a surface can be analyzed in great detail by looking at a large ensemble of molecules after a time, which is sufficient for the formation of the different intermediate and final states. If STM can be used to distinguish the individual intermediate states, a full reaction pathway can be unraveled. The relative occupation of the intermediate states may be compared to the prediction of a hypothesis, thereby verifying or dismissing models about the mechanism of the reaction, involved rates, activation energies etc. Once a model is developed, predictions for the reaction, like the temporal evolution of the intermediate states etc., can be made, e.g. for on surface synthesis or catalytic reactions. Since our approach does not require a high temporal resolution it may be directly applied to reactions of molecules on surfaces using standard scanning tunneling microscopy.

C.A.Bobisch acknowledges financial support from the Deutsche Forschungsgemeinschaft (DFG). ICN2 acknowledges support from the Severo Ochoa Program (MINECO, Grant SEV-2013-0295).

References

1 S. R. Crouch, J. Holler and D. A. Skoog, *Principles of Instrumental Analysis*, Brooks/Cole, 2006.
2 T. Waldmann, D. Künzel, H. E. Hoster, A. Gross and R. J. Behm, *Journal of the American Chemical Society*, 2012, **134**, 8817–8822.
3 J. Schütte, R. Bechstein, P. Rahe, H. Langhals, M. Rohlfing and A. Kühnle, *Nanotechnology*, 2011, **22**, 245701.
4 D. G. de Oteyza, P. Gorman, Y.-C. Chen, S. Wickenburg, A. Riss, D. J. Mowbray, G. Etkin, Z. Pedramrazi, H.-Z. Tsai and A. Rubio, *Science*, 2013, **340**, 1434–1437.
5 A. Riss, S. Wickenburg, P. Gorman, L. Z. Tan, H.-Z. Tsai, D. G. de Oteyza, Y.-C. Chen, A. J. Bradley, M. M. Ugeda and G. Etkin, *Nano letters*, 2014, **14**, 2251–2255.
6 J. Lu and K. P. Loh, *Angewandte Chemie International Edition*, 2013, **52**, 13521–13523.
7 L. E. Dinca, C. Fu, J. M. MacLeod, J. Lipton-Duffin, J. L. Brusso, C. E. Szakacs, D. Ma, D. F. Perepichka and F. Rosei, *ACS nano*, 2013, **7**, 1652–1657.
8 M. Treier, C. A. Pignedoli, T. Laino, R. Rieger, K. Müllen, D. Passerone and R. Fasel, *Nature chemistry*, 2011, **3**, 61–67.
9 M. Abel, S. Clair, O. Ourdjini, M. Mossoyan and L. Porte, *Journal of the American Chemical Society*, 2010, **133**, 1203–1205.
10 M. Matena, J. Björk, M. Wahl, T.-L. Lee, J. Zegenhagen, L. H. Gade, T. A. Jung, M. Persson and M. Stöhr, *Physical Review B*, 2014, **90**, 125408.
11 H. Marbach and H.-P. Steinrück, *Chemical Communications*, 2014, **50**, 9034–9048.
12 J. Wintterlin, S. VÃűlkening, T. Janssens, T. Zambelli and G. Ertl, *Science*, 1997, **278**, 1931–1934.
13 H. Wende, M. Bernien, J. Luo, C. Sorg, N. Ponpandian, J. Kurde, J. Miguel, M. Piantek, X. Xu and P. Eckhold, *Nature materials*, 2007, **6**, 516–520.
14 B. W. Heinrich, L. Braun, J. I. Pascual and K. J. Franke, *Nat Phys*, 2013, **9**, 765–768.
15 B. W. Heinrich, G. Ahmadi, V. L. Müller, L. Braun, J. Pascual and K. J. Franke, *Nano letters*, 2013, **13**, 4840–4843.

16 P. Sabatier, *The Method of Direct Hydrogenation by Catalysis. Nobel lecture, December 11, 1912. Nobel lectures in chemistry 1901-1921*, 1966.
17 X. Li, W. Cai, J. An, S. Kim, J. Nah, D. Yang, R. Piner, A. Velamakanni, I. Jung and E. Tutuc, *Science*, 2009, **324**, 1312–1314.
18 D. van Vörden, M. Lange, J. Schaffert, M. C. Cottin, M. Schmuck, R. Robles, H. Wende, C. A. Bobisch and R. Möller, *ChemPhysChem*, 2013, **14**, 3472–3475.
19 D. van Vörden, M. Lange, M. Schmuck, J. Schaffert, M. Cottin, C. Bobisch and R. Möller, *The Journal of chemical physics*, 2013, **138**, 211102.
20 H. C. Herper, M. Bernien, S. Bhandary, C. F. Hermanns, A. Krüger, J. Miguel, C. Weis, C. Schmitz-Antoniak, B. Krumme and D. Bovenschen, *Physical Review B*, 2013, **87**, 174425.
21 S. Arrhenius, *Zeitschrift für physikalische Chemie*, 1889, **4**, 226–248.
22 M. J. Powell, *The computer journal*, 1964, **7**, 155–162.